

Supplementary Information

Title: Machine learning-driven single-cell phenotyping in size-controlled microenvironments via parallel deterministic droplet microfluidics

Authors: Sangmin Lee^{1,2,3,4,5+}, Steven O'Donnell^{4,5+}, Zhangli Peng⁵, and Jae-Won Shin^{1,2,3,4,5*}

Affiliations

¹Department of Biologic and Materials Sciences & Prosthodontics, University of Michigan, Ann Arbor, MI, 48109

²Department of Biomedical Engineering, University of Michigan, Ann Arbor, MI, 48109

³Biointerfaces Institute, University of Michigan, Ann Arbor, MI, 48109

⁴Department of Pharmacology and Regenerative Medicine, University of Illinois at Chicago, Chicago, IL, 60612

⁵Department of Biomedical Engineering, University of Illinois at Chicago, Chicago, IL, 60607

+Equal contribution

*Correspondence to J.-W. S.: shinjaw@umich.edu

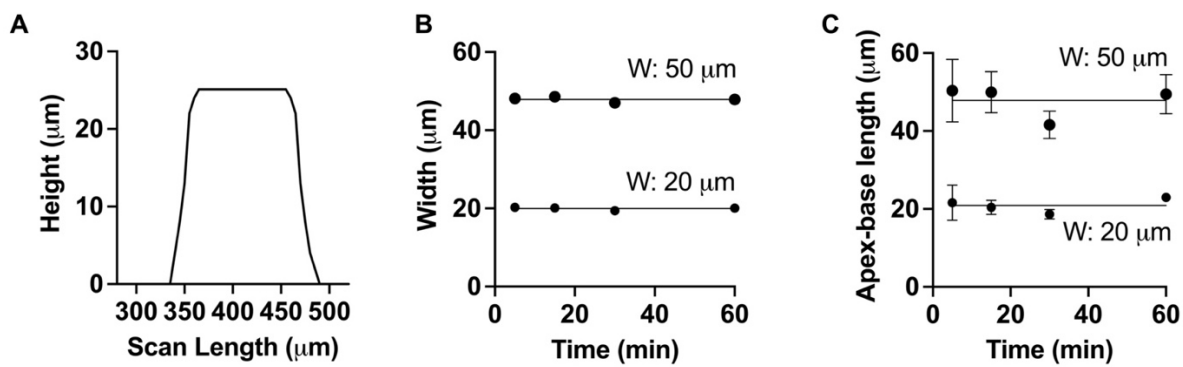


Figure S1. Characterization of microfluidic devices for parallel generation of multisized droplets. (A) SU-8 mold height measured by profilometry. (B) Width of PDMS junctions measured over 60 min of droplet generation. (C) Distance between the apex and base of droplets at junctions measured over 60 min of droplet generation.

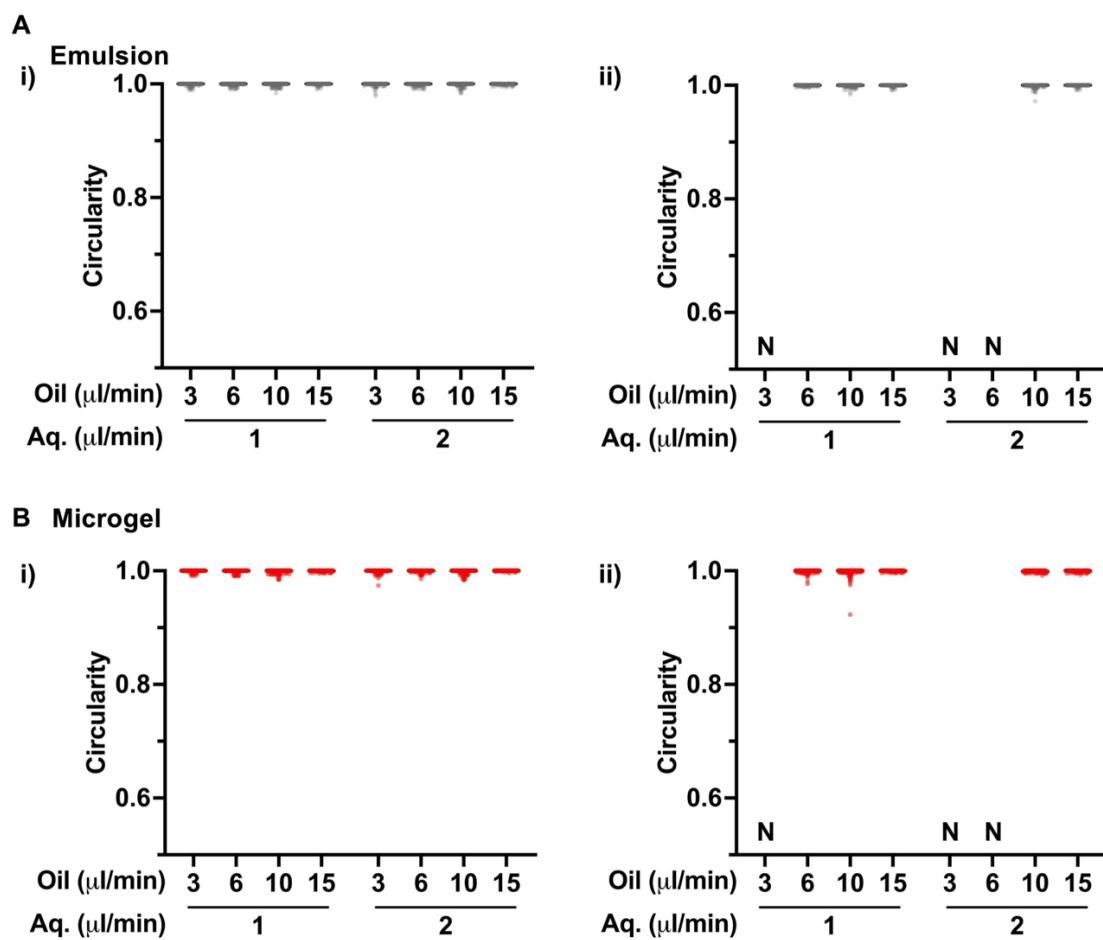


Figure S2. Measurement of droplet circularity. (A) Droplets in emulsion. (B) Crosslinked microgels following emulsion breaking. (i) 20 μm channel width; (ii) 50 μm channel width. ‘N’ indicates droplet not formed. $n = 100$ droplets per group.

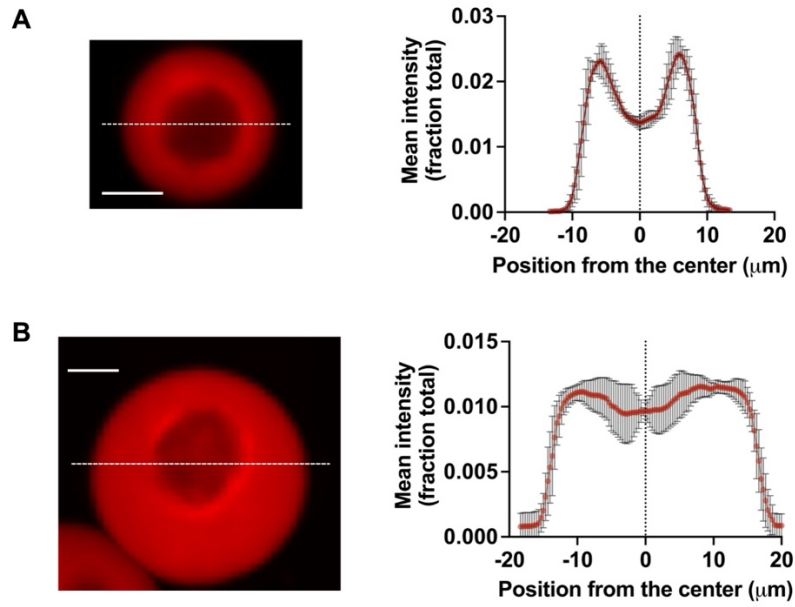


Figure S3. Distribution of crosslinked alginate across microgel shell thickness. Representative images and quantification of (A) small and (B) large microgels. Scale bar: 10 μm. $n = 5$ gel-coated cells per group. Error bars represent standard deviation.

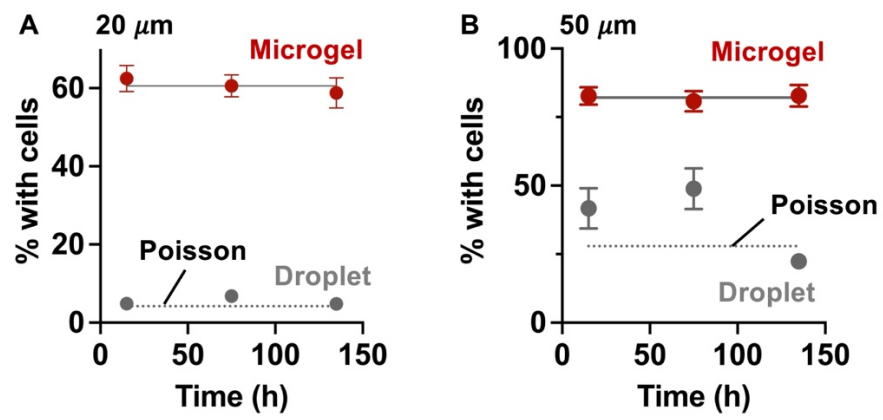


Figure S4. Fraction of cell-containing droplets and crosslinked microgels over time. (A) Small microgels. **(B)** Large microgels. Dotted lines indicate theoretical percentages based on Poisson statistics. $n = 3$ experiments. Error bars represent standard deviation.

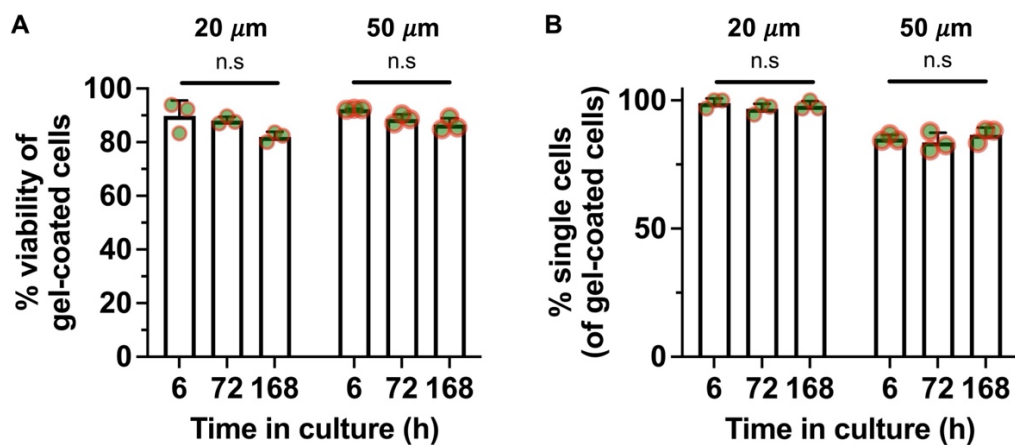


Figure S5. Assessment of gel-coated cells in culture. (A) Viability of gel-coated cells. **(B)** Fraction of single cells encapsulated in microgels relative to all gel-coated cells. $n = 3$ experiments. Error bars represent standard deviation.

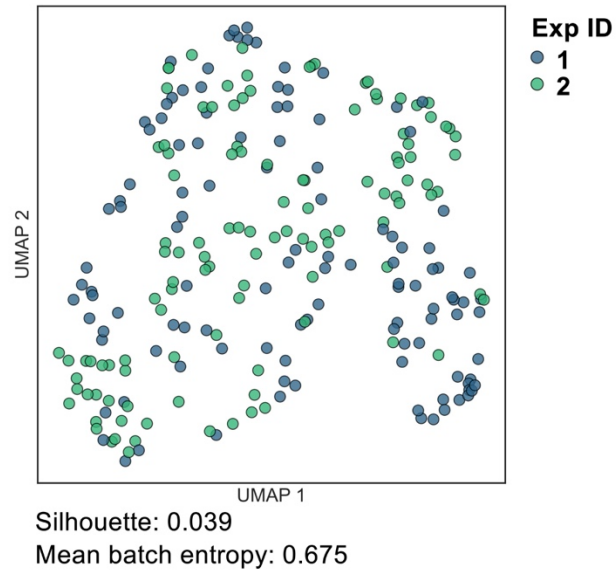


Figure S6. Quantification of cell population distribution across experiments. Silhouette scores (lower values indicate better mixing) and mean batch entropy values (higher values indicate better mixing) are shown.

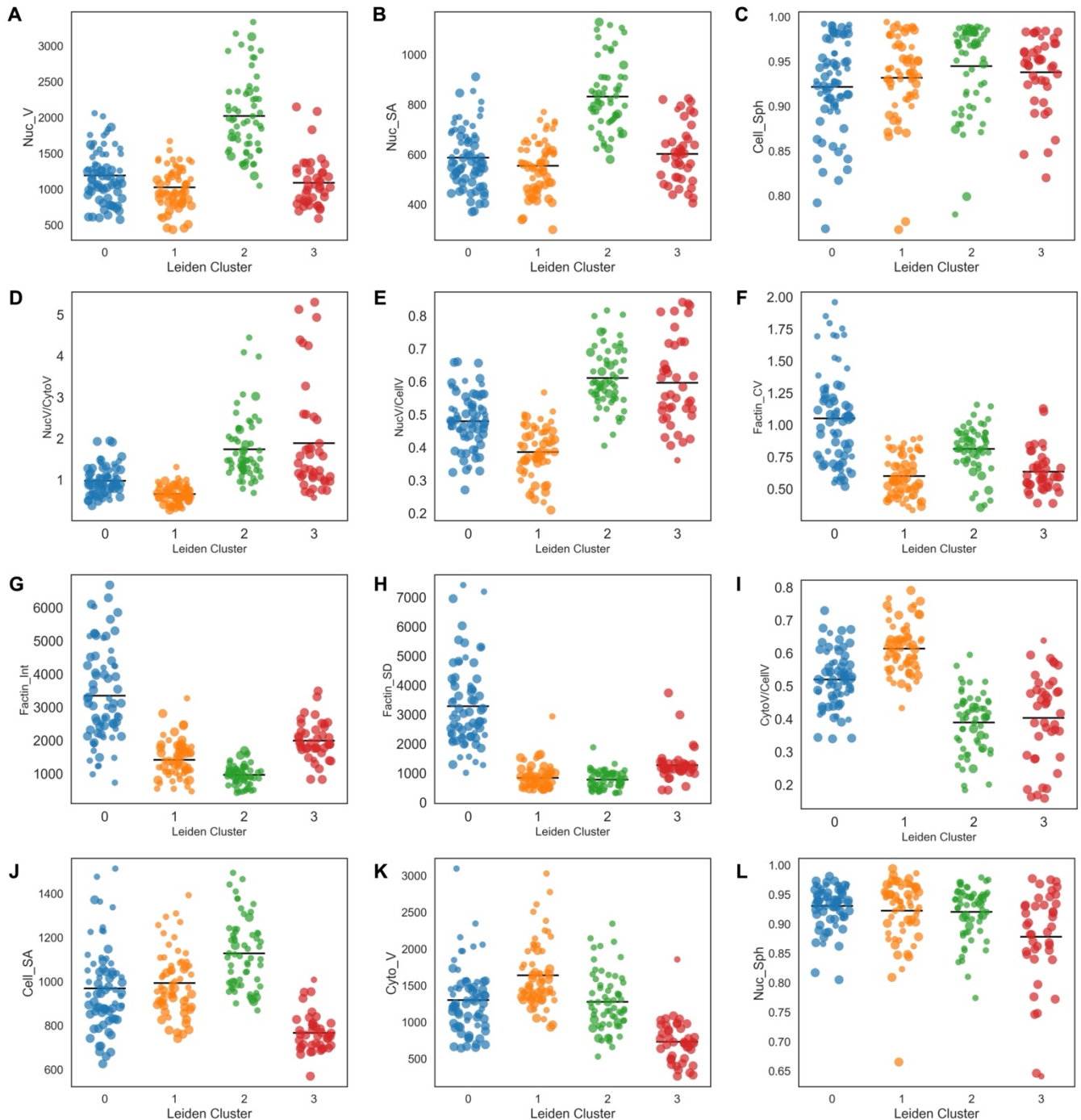


Figure S7. Quantification of phenotypic parameters for each cluster. (A) Nucleus volume (μm^3). (B) Nucleus surface area (μm^2). (C) Cell sphericity. (D) Nucleus-to-cytoplasm volume ratio. (E) Nucleus-to-cell volume ratio. (F) F-actin intensity coefficient of variation (CV). (G) F-actin mean intensity (a.u.). (H) F-actin intensity standard deviation (SD). (I) Cytoplasm-to-cell volume ratio. (J) Cell surface area (μm^2). (K) Cytoplasm volume (μm^3). (L) Nucleus sphericity. $n = 41$ - 69 gel-coated cells per group. All parameters were significantly different across clusters ($p < 0.05$, Welch's one-way ANOVA).

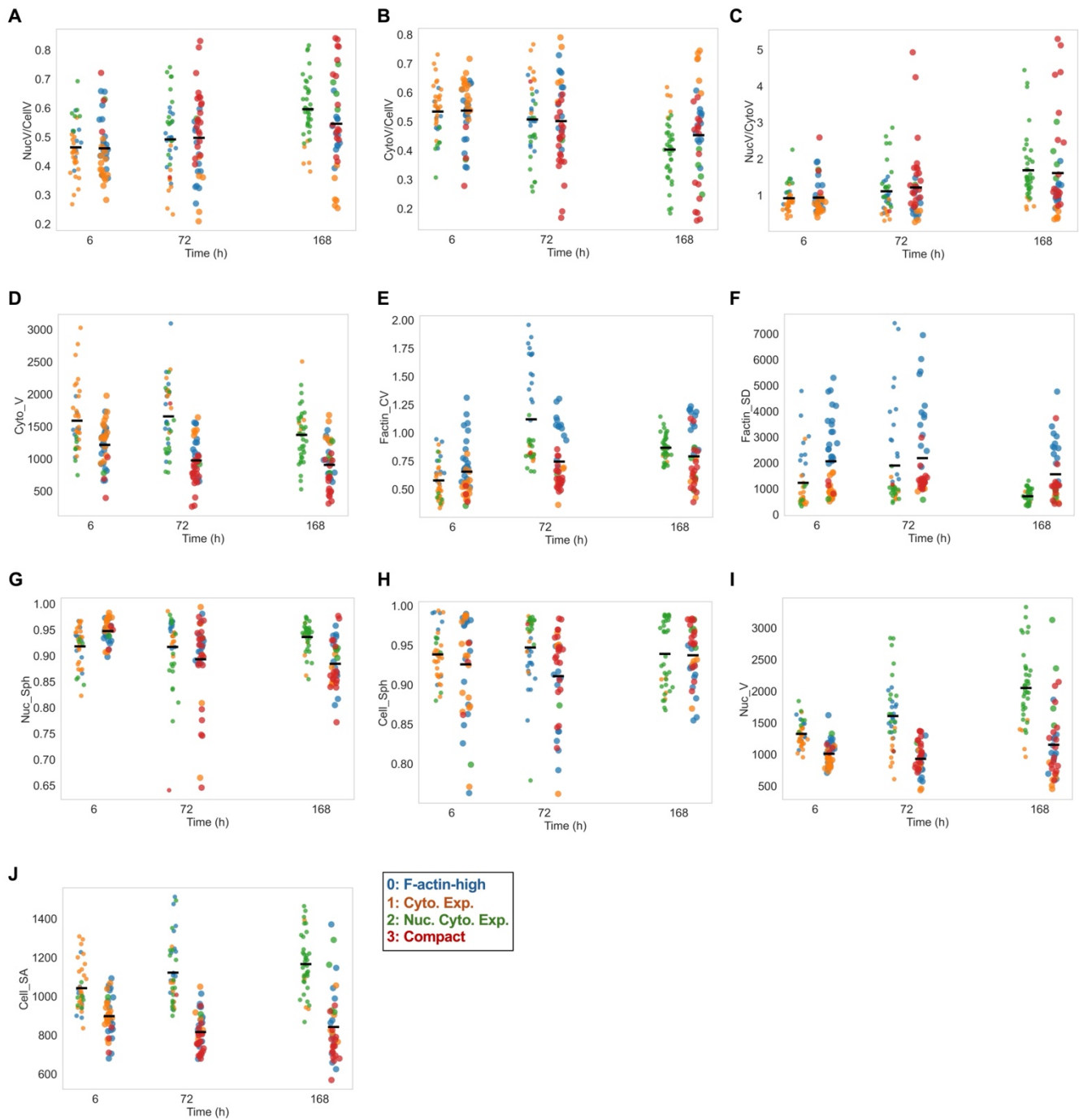


Figure S8. Quantification of phenotypic parameters across time points. (A) Nucleus-to-cytoplasm volume ratio. (B) Cytoplasm-to-cell volume ratio. (C) Nucleus-to-cell volume ratio. (D) Cytoplasm volume (μm^3). (E) F-actin intensity coefficient of variation (CV). (F) F-actin intensity standard deviation (SD). (G) Nucleus sphericity. (H) Cell sphericity. (I) Nucleus volume (μm^3). (J) Cell surface area (μm^2). Cells from different clusters are shown. $n = 37$ -40 per time point for each microgel size.